# Combinatorial Density Functional Theory-Based Screening of Surface Alloys for the Oxygen Reduction Reaction

**Jeff Greeley*,†,‡ and Jens K. Nørskov†**

*Center for Atomic-scale Materials Design, NanoDTU, Department of Physics, Technical University of Denmark, DK-2800 Kongens Lyngby, Denmark, and Center for Nanoscale Materials, Argonne National Laboratory, Argonne, Illinois 60439*

*Received: October 9, 2008; Revised Manuscript Received: December 30, 2008*

A density functional theory (DFT) -based, combinatorial search for improved oxygen reduction reaction (ORR) catalysts is presented. A descriptor-based approach to estimate the ORR activity of binary surface alloys, wherein alloying occurs only in the surface layer, is described, and rigorous, potential-dependent computational tests of the stability of these alloys in aqueous, acidic environments are presented. These activity and stability criteria are applied to a database of DFT calculations on nearly 750 binary transition metal surface alloys; of these, many are predicted to be active for the ORR but, with few exceptions, they are found to be thermodynamically unstable in the acidic environments typical of low-temperature fuel cells. The results suggest that, absent other thermodynamic or kinetic mechanisms to stabilize the alloys, surface alloys are unlikely to serve as useful ORR catalysts over extended periods of operation.

## Introduction

The first examples of the use of computational, density functional theory (DFT) -based approaches to screen for improved heterogeneous catalysts have recently appeared in the literature.[1−9] These screening studies have resulted in the identification of leads for improved catalysts for reactions of interest in the processing and cleanup of hydrocarbon streams,[4,7,8] the preferential oxidation of CO in hydrogen,[9] and hydrogen production/evolution in low-temperature fuel cells,[1] among others. These studies have convincingly demonstrated that first-principles catalyst design is now a reality, but they have also pointed to the tremendous challenge associated with identifying catalytic alloys that are not only active but also stable for reactions of interest. This challenge is expected to be particularly acute for chemical reactions that occur in aqueous electrochemical environments at high electrode potentials when the twin processes of metal dissolution and surface oxide formation are expected to occur readily.

The oxygen reduction reaction (ORR) occurs in electrochemical environments under conditions of high electrode potential and is, thus, expected to be susceptible to the stability issues mentioned above. Indeed, recent reports have highlighted the importance of stability considerations in the identification of improved ORR catalysts.[10,11] Previous computational treatments of this reaction have either not considered stability issues or have restricted their analyses to alloys containing significant quantities of platinum or palladium, materials that are known to be kinetically stable in electrochemical systems over relatively long periods of operation.[12,13] Hence, in spite of the significant technological interest in finding ORR catalysts superior to pure platinum,[14] an extensive computational search for improved ORR catalysts that explicitly incorporates catalyst stability criteria has yet to be performed.

In the present study, we present a combinatorial, fully DFT-based, computational heterogeneous catalyst screening effort to identify improved ORR catalysts. We explicitly consider potential-influenced stability phenomena in our study, and we thus employ a screening procedure that efficiently combines catalytic activity criteria, the indicated stability assessments, and a database of density functional theory calculations on nearly 750 binary transition metal surface alloys. We find that, although a large number of alloys are predicted to have high activity for the ORR, very few such alloys are expected to be thermodynamically stable at high electrode potentials. The results suggest that, over extended periods of operation, very few surface alloys are likely to possess sufficient stability to serve as ORR catalysts, and the well-studied Pt and Pd bulk alloy "skin" structures may, indeed, be among the only alloys that will be both active and stable for the ORR.[11]

## Methods

The DACAPO code[15] is used for all total energy calculations in this study. A three-layer slab, periodically repeated in a super cell geometry with five equivalent layers of vacuum between any two successive metal slabs, is used. A $(\sqrt{3} \times \sqrt{3})R30°$ unit cell, corresponding to an adsorbate coverage of $^1/_3$ ML, is employed. The majority of slabs are constrained to a face-centered cubic (fcc) crystal structure with lattice constants optimized for that crystal system; however, three metals that are naturally hexagonal close-packed (hcp) (Ru, Re, and Co) are treated in that structure. This procedure will introduce modest inaccuracies into calculations for alloys where Fe, Cd, As, Sb, and Bi (whose natural crystal structures are non-fcc) form the substrate (see description of alloy geometries below). However, it will not significantly affect the results for alloys wherein these elements are present only in the surface layer, and it is the latter group of alloys that turn out to be more interesting for the ORR. The slabs are kept fixed in their bulk-truncated geometries, and the oxygen adsorbate (located at fcc, hcp, or top sites) is relaxed according to the Hellman−Feynman forces until the total force on the oxygen atom is less than 0.6 eV/Å (the average residual

* To whom correspondence should be addressed: phone (630) 252-4711; fax (630) 252-4646; e-mail jgreeley@anl.gov.
† Technical University of Denmark.
‡ Argonne National Laboratory.

10.1021/jp808945y CCC: $40.75 
Published on Web 03/03/2009

forces are substantially less than this value). The total energy is then further refined by using the residual forces and estimated harmonic vibrational frequencies for oxygen (~510 $cm^{-1}$ for 3-fold sites and ~770 $cm^{-1}$ for top sites) to extrapolate to the bottom of a parabola in energy space; these corrections typically amount to a few hundredths of an electronvolt. The net analysis typically gives binding energies within ~0.1 eV of the most accurate values, completely adequate to reveal semiquantitative trends in the activities of the alloys under consideration; we note that a similar approach has been used successfully to screen for catalysts where hydrogen adsorption determines the descriptor value.[1] The calculated binding energies are similar to those reported in a previous study,[16] although a different force convergence criterion was used in that work.

Adsorption is allowed on only one of the two exposed surfaces of the metal slabs, and the electrostatic potential is adjusted accordingly.[17] Ionic cores are described by ultrasoft pseudopotentials,[18] and the Kohn−Sham one-electron valence states are expanded in a basis of plane waves with kinetic energy below 340 eV; a density cutoff of 500 eV is used. The surface Brillouin zone is sampled with an $18(\sqrt{3} \times \sqrt{3})$ Chadi−Cohen **k** point grid. In all cases, convergence of the total energy with respect to the cutoff energies and the **k** point set is confirmed. The exchange−correlation energy and potential are described by the generalized gradient approximation (GGA-RPBE).[15] The self-consistent RPBE density is determined by iterative diagonalization of the Kohn−Sham Hamiltonian, Fermi population of the Kohn−Sham states ($k_BT = 0.1$ eV), and Pulay mixing of the resulting electronic density.[19] All total energies have been extrapolated to $k_BT = 0$ eV. Zero-point energy effects are assumed to be approximately constant for all metals and alloys considered.[20] Spin polarization effects are included in the reported results for alloys in which naturally magnetized metals (Ni, Co, Fe) are present.

Potential-dependent free energies of oxygen adsorption are determined by a procedure introduced in previous work.[20,21] In those studies, it was determined that addition of a water bilayer has no effect on the binding energy of atomic oxygen, and solvation effects on oxygen binding are therefore neglected in the present study. Potential effects (versus SHE) are included by adjusting the free energies of adsorption (per transferred electron) by −eU. Appropriate zero-point energy and entropy corrections are also applied, as defined in the previous publications.

The binary transition metal surface alloys considered in this study consist of one surface layer and two substrate layers. These alloys are described with the notation ABCD; in this formalism, A, B, and C denote the elemental nature of the three atoms in the surface layer while D indicates the identity of the element in the substrate layer; the lattice constant of the alloy is dictated by the lattice constant of the substrate element. In total, binary combinations of 16 elements (Fe, Co, Ni, Cu, Ru, Rh, Pd, Ag, Ir, Pt, Au, Re, Cd, As, Sb, and Bi) are considered; these metals were chosen because they are not thermodynamically favored to form bulk oxides in water at zero applied potential versus the standard hydrogen electrode (SHE) and because they represent a broad spectrum of catalytically interesting elements.

## Results and Discussion

A general, descriptor-based strategy for high-throughput computational catalyst screening has been outlined previously.[1,2] Briefly, this approach involves first finding a set of descriptors (binding energies, activation barriers, etc.) that, when combined with simple reactivity models, reliably predicts trends in the catalytic activities. These descriptors are then evaluated, by use of DFT, on a large set of alloys, and the alloys with the highest predicted activity are selected for further analysis. Each of the selected alloys is then subjected to series of computational stability tests; as mentioned above, such considerations are of first-order importance when dealing with electrochemical processes occurring at high potentials. Any alloys that are predicted to be thermodynamically unstable with respect to any of the considered stability phenomena are eliminated from consideration, yielding a pool of computationally optimized candidates. This scheme is quite efficient and permits estimation of the activity and stability of a large number of transition metal alloys with reasonable computational effort. Below, we illustrate the application of this very general approach to the oxygen reduction reaction.

**ORR Descriptors on Transition Metal Alloys.** Previous studies have established that a volcano-shaped curve is formed when the activity of catalysts for the ORR (as determined by an appropriately normalized logarithm of the calculated reaction rate) is plotted against a measure of the catalysts' affinity for oxygen. Sabatier analysis (a simplified form of microkinetic rate theory yielding an upper bound to the rate) has demonstrated that the binding energy of either atomic oxygen ($\Delta E_O$) or hydroxyl is a useful descriptor for this reaction.[20,21] A value of $\Delta E_O$ slightly more positive than that of pure platinum (corresponding to slightly weaker binding), the best pure metal for the ORR, is predicted to yield optimal catalytic activity. DFT-based calculations of $\Delta E_O$, in turn, have been shown to accurately predict which metals and alloys lie near the optimum of this volcano; indeed, calculations of platinum-based alloys have yielded activity trends in excellent agreement with experimental results,[21,22] further supporting the use of $\Delta E_O$ as a descriptor for the ORR.

**Evaluation of the Descriptor on Transition Metal Alloys.** The usefulness of the oxygen binding energy as an ORR descriptor implies that a fruitful computational search for new ORR catalysts might begin with the determination of $\Delta E_O$ on a large number of transition metals and alloys. To this end, oxygen binding energies on 736 binary transition metal surface alloys have been determined with DFT calculations. The resulting values are shown schematically in Figure 1, and the data are tabulated in Table S1 in Supporting Information.

In a previous study of oxygen binding to transition metal surface alloys,[16] we developed an interpolative model for oxygen binding energies based on the surface *d*-band center.[23] In the present work, our primary goal is not to further analyze trends in oxygen binding energies but rather to use binding energy data to find active and stable catalysts for the ORR. For that reason, we present only a brief discussion of the main features of Figure 1. In the indicated figure, we have plotted the deviations of the oxygen binding energies on all 736 surface alloys considered in this study from the value of $\Delta E_O$ that gives the optimal predicted ORR activity at a potential of 0.9 V versus SHE (the optimal value is 0.2−0.25 eV more positive than that of pure Pt;[21] a value of 0.22 eV is used in the present analysis).

In general, alloys wherein the solute is a late-group transition metal have $\Delta E_O$ values closer to the optimal value than do alloys with early group solutes; this behavior is likely related to the fact that early group transition metals (Fe, Co, Ni, Ru, Rh, Re, etc.) bind oxygen too strongly to be active for the ORR.[20] At low solute coverages ($^1/_3$ ML), however, a limited number of surface alloys containing early group solutes actually have favorable predicted ORR activities. These solutes are alloyed onto substrates that bind oxygen weakly, and the favorable ORR

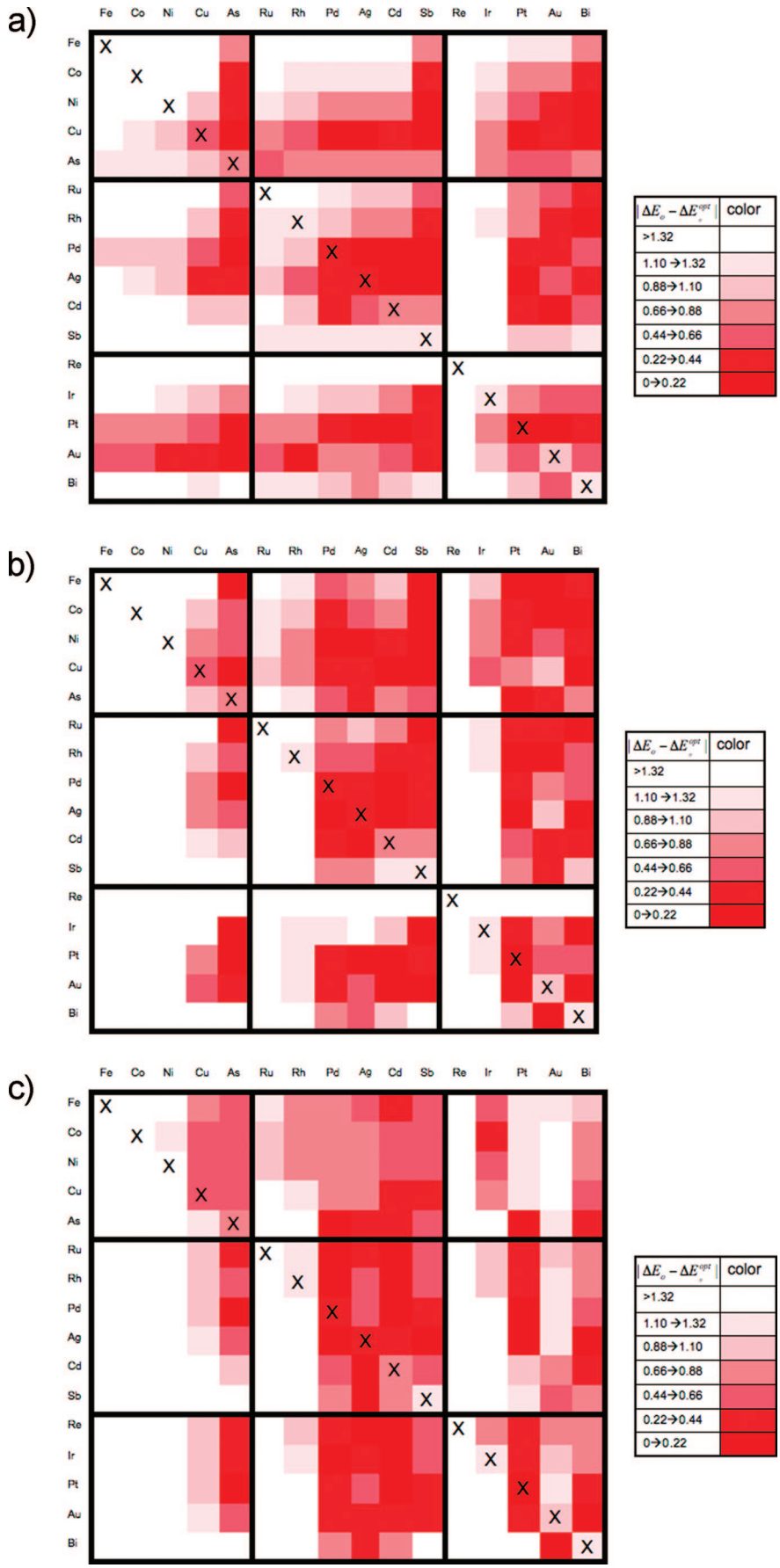


**Figure 1.** Deviations of the oxygen binding energy ($\Delta E_O$) from the binding energy that gives optimal predicted ORR activity at 0.9 V vs SHE; the latter value is taken to be ~0.22 eV more positive than the calculated $\Delta E_O$ for pure platinum at $T = 298$ K and pH = 0. $\theta_O = {}^1/_3$ML. Coverage of solute elements (columns) in the surface layer of host elements (rows) is (a) ${}^1/_3$ ML, (b) ${}^2/_3$ ML, and (c) 1 ML. An × on the diagonal denotes a pure element.

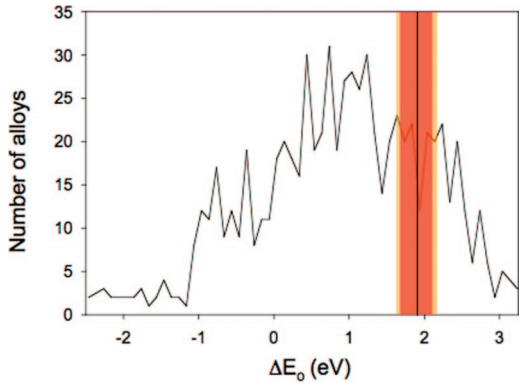


**Figure 2.** Histogram depicting the oxygen binding energies ($\Delta E_O$) of 736 binary surface alloys. The vertical line denotes the value of $\Delta E_O$ that is predicted to give the highest activity at a potential of 0.9 V vs SHE. The shaded red area corresponds to those alloys that are predicted to be at least as active as pure platinum, and the shaded orange area is the corresponding region for pure palladium.

properties simply reflect an averaging of the oxygen binding energies of the solute and the host, both of which are present in the surface layer of the alloy; this effect is consistent with the interpolation principle of adsorbate binding energies.[4,16] An example of such an alloy is Ni/Au; in that case, although Ni binds oxygen very strongly, the surface alloy is predicted to have reasonable ORR activity. At higher solute coverages, these interpolative effects largely disappear, and, as mentioned above, surface alloys with early group solutes are seen to bind oxygen too strongly to be of interest for this reaction. Finally, we note that there is a somewhat surprising tendency for surface alloys with overlayers of large solutes (As, Sb, Bi, Cd, etc.) to show favorable oxygen binding properties for the ORR. These solutes are known to be too oxophilic in their pure forms to be interesting for the ORR, but when present as solutes in surface alloys, they become highly compressed since they are forced to adopt the (generally smaller) lattice constant of the substrate. This compression, in turn, leads to a significant weakening of oxygen binding in the surface alloy compared to the pure solute,[24,25] yielding a more favorable predicted ORR activity. We note, however, that the compression of pure monolayers of these solutes may ultimately result in sufficiently large compressive forces to induce surface reconstruction.

Of the 736 surface alloys considered, 85 are predicted to be at least as active as pure Pt for the ORR, and 111 are predicted to be more active than pure Pd. These active alloys are depicted schematically by the shaded regions of Figure 2, a histogram of the oxygen binding energies on all surface alloys in the present study; the active alloys are natural candidates for further analysis.

**Stability Analysis of Alloys.** The tabulated values of $\Delta E_O$ in Figure 1 and Table S1 (Supporting Information), together with the shaded regions of the histogram in Figure 2, demonstrate that a significant number of binary surface alloys have high predicted activity for the oxygen reduction reaction. However, it is well-known that a large number of pure metals and alloys become unstable in the highly oxidizing, high-potential, corrosive environments that are associated with ORR operating conditions.[10,14] Hence, for the present theoretical screening effort to be useful, it is essential to develop a means of filtering out these unstable systems. Herein, we extend a basic stability analysis, introduced previously,[2] to ORR environments. We consider several mechanisms by which the surface alloys of high predicted activity might become unstable in such environments, including surface segregation, surface islanding, oxide formation, and metal dissolution (see Figure 3); for each possible destabilization mechanism, we explicitly include the effect of potential-induced oxygen adsorption on the indicated process.

The simplest stability test deals with surface segregation.[26] For certain of the alloys under consideration, either with or without adsorbed oxygen, it will be thermodynamically favorable for substrate atoms to displace solute atoms in the surface (the solute atoms will subsequently move into the bulk). We evaluate these thermodynamics for a variety of segregation events that could occur for each surface alloy of high predicted activity, both with and without adsorbed oxygen on the resulting segregated slabs, and we eliminate from consideration alloys that are not stable in the electrode potential range of interest for the ORR; this procedure is similar to that introduced previously for the hydrogen evolution reaction.[1,2] We consider only segregation processes that result in the formation of surface alloys that are already present in our database and, using the approach described in the Appendix, we determine the free energy change for each considered segregation process as a function of the electrode potential. Several stability regimes can be identified from this analysis; for example, if both the clean surface and the oxygen-covered surfaces of the alloy under consideration have lower free energies than the respective clean and O-covered surfaces of all possible segregated slabs, then segregation will not occur at any electrode potential. Conversely, if both the clean and O-covered slabs are less stable than the corresponding segregated slabs, then segregation will be thermodynamically favorable at all potentials. If the initial clean slab is more stable than the segregated clean slabs, yet oxygen adsorption renders the segregated slabs more stable, then oxygen-induced segregation will occur when the potential becomes sufficiently high. Finally, if the initial clean slab is less stable than the segregated clean slabs but the O-covered initial slab is more stable than the corresponding segregated systems, oxygen-induced desegregation will occur at sufficiently high potentials. By considering each of these segregation-related stability regimes for all surface alloys of high predicted activity, we effectively produce a complete phase map of the free energy of these alloys (and associated segregated alloys) as a function of the electrode potential. We use this information to eliminate from consideration those surface alloys that are not thermodynamically stable with respect to segregation in the potential range of interest for the ORR (~0.4−0.9 V). Fifty-seven alloys are eliminated in this manner, and the eliminated alloys are generally characterized by one of three features: a positive segregation energy in vacuum (implying that the solute has a thermodynamic preference for diffusion into the bulk; for example, PtPtPtAu), a high surface coverage of solute atoms with large atomic radii and non-fcc crystal structures (thus introducing significant strain/deformation energy into the surface layer and thereby favoring diffusion of solute into the bulk; for example, BiBiBiAg), or a much stronger binding of oxygen to the substrate element than to the solute (leading to oxygen-induced segregation; for example, CoPtPtCo).

The second stability test concerns phase segregation that is primarily within the surface layer of the alloys. Even if solute elements do not segregate into the bulk, they may still undergo purely surface-localized rearrangements (e.g., so-called "islanding" rearrangements). To analyze these types of intrasurface instabilities, we calculate the free energy change, in both the presence and the absence of adsorbed oxygen, associated with several possible rearrangements for each surface alloy (see Appendix for additional details); we also consider the possibility

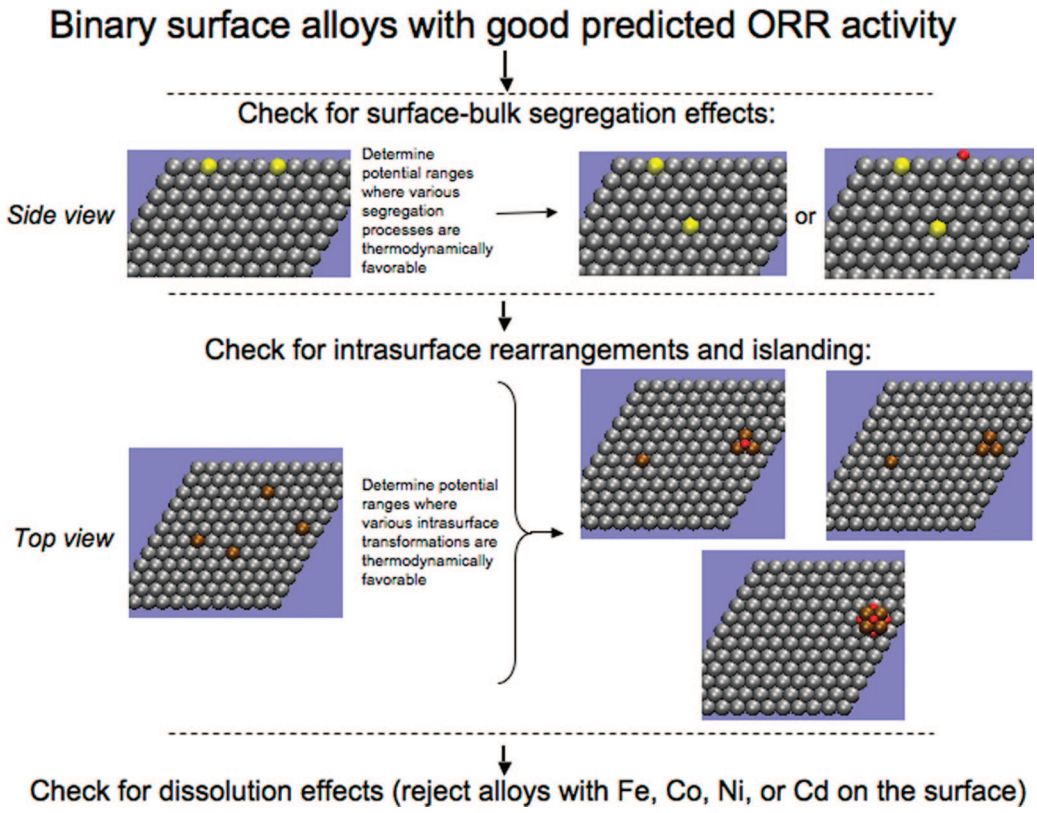


**Figure 3.** Schematic representation of surface alloy stability tests. Red circles denote adsorbed oxygen, yellow and ochre circles denote solute metal atoms, and silver circles denote host metal atoms. Not all stability tests considered in the text are depicted in the schematics. The graphics were produced with VMD.[35]

that localized patches of bulk metal oxides may form as a result of surface-localized rearrangements. We consider only destabilization processes that result in the formation of bulk oxides or in alloys that are present in our full database. As with the stability analysis for segregation, we produce a complete phase map (free energy versus electrode potential) of the surface alloys and associated islanding-type rearrangements, and we eliminate from consideration any alloys that are thermodynamically unstable with respect to such rearrangements in the potential range of interest for the ORR. Twenty-five alloys are found to be unstable at all potentials, and an additional 17 become unstable at low potentials (below 0.4 V). Factors quite similar to those found in the case of segregation-related destabilization seem to control the surface-localized rearrangements; surface alloys with full monolayer coverages of large solutes on smaller substrates are susceptible to such rearrangements, as are alloys with large differences between the oxygen binding energies (or the free energies of bulk oxide formation) of the solutes and the substrates.

The final stability test involves the tendency of surface atoms to dissolve in the acidic environments often associated with ORR operation. The thermodynamic driving force for such stripping can be evaluated from the electrochemical series, taking the lowest dissolution/stripping potential of all elements present in the surface layer (no experimental values are available for As and Sb, and direct dissolution of these species in ionic form is not considered);[27] of the 16 elements considered in this study, Fe, Co, Ni, and Cd are expected to dissolve readily in acid at pH = 0. Hence, it is unlikely that any alloys with these elements in the surface layer will be stable in acidic oxygen reduction environments, and such alloys are eliminated from consideration. We note, in passing, that although this simple stability criterion suggests that surface alloys with these elements in the surface layer will never be suitable ORR catalysts in acidic environments, it is possible that they could be useful in nonacidic media. It is also likely that more complex criteria (accounting for the effect of alloying on the dissolution potentials) would demonstrate that some of them are, in fact, stable to potentials higher than the bulk dissolution potentials of the pure component elements.

Additional stability tests for ORR catalysts could, conceivably, be performed. However, the above tests capture the first-order effects of surface rearrangements, electrode potential, oxide formation, and dissolution on surface alloy stability, and they should be sufficient to eliminate the most unrealistic alloys from consideration. There is thus a good probability that any candidates that survive these tests will be stable in real ORR environments.

**Stable, Active Oxygen Reduction Catalysts.** In Table 1, the alloys that are predicted to be most active and stable for the ORR are listed. Although these 29 surface alloys and pure metals represent the most interesting candidates from our original pool of 736 alloys, even this list does not suggest any candidates that are likely to survive extended operation at elevated potentials (~0.9 V), particularly when potential cycling occurs.[28] Seventeen of the alloys will become unstable if the potential rises above a maximum of ~0.35 V, the dissolution potential of bulk Cu (a species that is notorious for rapid corrosion in acidic environments[29]). Eight candidates (containing primarily Pt, Pd, Ag, or group VA elements in the surface layer) will survive above 0.5 V. Even this level of stability, however, may not be sufficient to yield robust catalysts capable of long-term operation in fuel cells.

The results of our activity and stability analyses strongly suggest that, while numerous surface alloys may be active for the ORR, only a tiny fraction of that number will likely be stable

**TABLE 1: Stability Analysis of ORR Alloys with High Predicted Activity[a]**

| Surface alloy or metal | Deviation from optimal ORR value (eV) | Segregation potential | Surface phase separation potential | Dissolution potential |
|---|---|---|---|---|
| PtPtPtPt | −0.22 | "nf" | "nf" | 1.18 |
| PdPdPdPd | −0.27 | "nf" | "nf" | 0.95 |
| PdPdSbPd | 0.16 | 0.92 | 0.78 | 0.95 |
| PdPdAgPd | 0.05 | 0.86 | 0.76 | 0.80 |
| PdPdAsPd | −0.15 | "nf" | 0.66 | 0.95 |
| PtPtSbPt | 0.24 | 1.06 | 0.62 | 1.18 |
| RhPtPtRh | −0.18 | 0.73 | 0.57 | 0.60 |
| PtPtPtIr | 0.24 | "nf" | 0.51 | 1.18 |
| RhRhSbRh | −0.27 | 0.74 | 0.44 | 0.60 |
| PtPtAsPt | 0.04 | 0.95 | 0.41 | 1.18 |
| RuPtPtRu | −0.25 | "nf" | 0.39 | 0.46 |
| PtPtPtRu | 0.27 | "nf" | 0.39 | 1.18 |
| CuCuPtCu | 0.08 | 0.74 | 0.46 | 0.34 |
| CuCuPdCu | −0.13 | 0.70 | 0.46 | 0.34 |
| CuCuAsCu | −0.11 | "nf" | 0.36 | 0.34 |
| RhRhBiRh | −0.12 | "nf" | 0.36 | 0.31 |
| RuAsAsRu | 0.07 | "nf" | 0.31 | 0.46 |
| PdPdPdRu | 0.09 | "nf" | 0.23 | 0.95 |
| CuCuSbCu | −0.02 | "nf" | 0.21 | 0.34 |
| IrAsAsIr | −0.22 | "nf" | 0.21 | 1.16 |
| AgAgSbAg | 0.00 | "nf" | 0.18 | 0.80 |
| AgAgAsAg | −0.22 | "nf" | 0.15 | 0.80 |
| AsAsAsIr | 0.25 | "nf" | 0.09 | "nf" |
| PdPdPdRe | 0.26 | 0.82 | 0.09 | 0.95 |
| NiNiSbNi | −0.16 | 0.84 | 0.01 | −0.26 |
| AgAgCdAg | 0.12 | "nf" | 0.15 | −0.40 |
| AgCdCdAg | −0.07 | "nf" | 0.08 | −0.40 |
| FeAsAsFe | 0.17 | 0.60 | −0.21 | −0.45 |
| FePtPtFe | −0.05 | 0.19 | −0.24 | −0.45 |

[a] Entries are ordered from highest to lowest stability. "Deviation from optimal ORR value" is the difference between the calculated oxygen binding energy and the optimal binding energy for the ORR at 0.9 V vs SHE (in eV). "Segregation potential and surface phase separation potential" correspond to the electrode potential (in V vs SHE) at which the particular segregation or surface phase separation process that is most likely to destabilize each alloy becomes thermodynamically favorable; "nf" indicates that the given tranformation is not thermodynamically favorable at any potential. The "dissolution potential" is taken from the electrochemical series (no experimental dissolution potentials are available for As and Sb). Determination of these free energy values is described in detail in the text and in the Appendix. Complete lists of calculated oxygen binding energies are given in Table S1 (Supporting Information).

in the challenging conditions under which ORR catalysts typically operate. Although this conclusion seems inescapable, given our results, we note that our stability analyses are quite conservative, and in reality, some of the candidates that we have excluded from consideration for stability reasons might, in practice, serve as effective ORR catalysts, at least over limited periods of operation. In particular, all of our stability criteria are thermodynamic in nature; at the low temperatures that characterize proton exchange membrane (PEM) fuel cell operation, it might be true that some of the surface alloy candidates are *kinetically* stable, even if thermodynamics argue against their long-term survival.[12,30] For example, a number of the surface alloys in Table 1 contain group VA elements (As, Sb, or Bi); we find that these alloys are nearly all destabilized by formation of bulk group VA oxides. If there is a significant kinetic barrier to such bulk oxide formation, however, then the alloys will be stable to much higher potentials (over 1 V, in many cases). Additionally, in general, if the ORR is run at lower potentials (higher overpotentials), then additional alloys will become thermodynamically stable.

The conclusion that potential-induced destabilization phenomena will render most binary surface alloys unsuitable for long-term ORR operation, even when the predicted ORR activity of these alloys is very high, underlines the importance of incorporating potential-induced stability criteria into screening efforts for ORR catalysts. The present results also further motivate the investigation of bulk alloy Pt and Pd skins as ORR catalysts.[11,22] The skins on these bulk alloys may be stabilized by the underlying alloy[31] and can effectively protect the underlying base metals from the harsh ORR environments, permitting long-term operation. Such skinlike structures are, perhaps, the only materials that offer a realistic hope of having greater activity than pure Pt and are a worthy subject of future study.

## Conclusions

A general procedure for fully density functional theory-based screening of binary surface alloys (systems consisting of a solute metal alloyed into the surface layer of a homogeneous host metal) has been used to search for improved oxygen reduction reaction catalysts. Application of descriptor-based activity criteria to a large database of transition metal surface alloys (∼750 systems) shows that many such alloys have high predicted activity for the ORR. However, subsequent application of rigorous, potential-dependent stability tests to the alloys of highest predicted activity shows that nearly all promising candidates will be thermodynamically unstable at the high potentials associated with the ORR. This result implies that binary surface alloys are not likely to be suitable candidates for long-term use as ORR catalysts unless additional mechanisms can be identified to stabilize these materials. It should be stressed, however, that future extension of these studies to include bulk alloys and surface alloys with more alloying components would likely yield more promising catalysts. We have already found, for example, that the improved ORR activity of bulk Pt alloys with a number of 3d transition metals, where Pt has segregated to the surface, can be described by the present

formalism. It is therefore likely that this formalism can be used to search such systems more systematically and to identify promising ORR catalysts that are both active and stable in realistic fuel cell operating conditions.

**Acknowledgment.** Use of the Center for Nanoscale Materials at Argonne National Laboratory was supported by the U.S. Department of Energy, Office of Basic Energy Sciences, under Contract DE-AC02-06CH11357. J.G. acknowledges a H. C. Ørsted Postdoctoral Fellowship from the Technical University of Denmark. The Center for Atomic-scale Materials Design is supported by the Lundbeck Foundation. We thank the Danish Center for Scientific Computing for computer time. We also acknowledge computer time at the Laboratory Computing Resource Center (LCRC) at Argonne National Laboratory.

## Appendix

In this appendix, details relating to two of the stability analyses that are applied to binary surface alloys, surface segregation and surface-localized (intrasurface) phase separation, are given. A third stability analysis, describing the leaching of atoms in acidic solutions, is fully described in the text.

Surface segregation stability analyses are performed by use of a grand canonical free energy formalism. The use of free energy approaches, both with and without an applied electrode potential, to understand surface phase diagrams and the surface stability of monometallic systems has been described in the literature (see, for example, refs 32 and 33). In the present study, the free energies (on a per-unit cell basis) of various surface configurations are compared: the alloy whose stability is being assessed (both with and without adsorbed oxygen), different oxygen-covered alloys (at $\theta_O = {}^1/_3$ ML) that result from segregation of surface atoms to the bulk (generally speaking, there are multiple such segregation events that can occur for any given alloy), and the corresponding surface-segregated alloys without adsorbed oxygen. To keep the analysis tractable, we consider only final, segregated states that are found in our database of 736 surface alloys; hence, all stability calculations use the same force convergence criteria as are described for the calculations in the Methods section. The free energies are calculated as differences of total energies and electrode potential-dependent oxygen chemical potentials (surface entropy effects are neglected).[34] To preserve candidates in the analysis that might be only slightly unstable (well within the error bars of our calculations), we subtract 0.05 eV from the initial clean slab total energies (this procedure is used both in this analysis and in the surface phase separation analysis). Adsorbed oxygen is assumed to be in equilibrium with bulk water, and its chemical potential changes according to the electrode potential (calculated against the standard hydrogen electrode, or SHE); the formalism, and associated entropy parameters used in the present study, are described in detail in ref 20. Total energies are evaluated from DFT calculations and from a database of calculated surface segregation energies (the latter is defined as the energy required to move an isolated atom of solute from the bulk to the surface of a host material). Surface segregation energies in the database account fully for the effect of solute coverage; the detailed determination of these energies is described elsewhere.[2] Once the potential-dependent free energies of the surface alloy under consideration (both with and without adsorbed oxygen), together with the corresponding quantities for the relevant segregated slabs, are determined, the electrode potential range in which the initial surface alloy is stable is straightforwardly identified.

Intrasurface phase separation stability analyses are performed in a similar manner. The free energies of numerous surface configurations that could result from intrasurface phase separations of the alloy of interest are compared. All separations that result in two surface alloys with the same substrate and with the same overall stoichiometry as the original alloy (again, with the restriction that the separated alloys must also be in our database), together with rearrangements of the initial alloy into phases of bulk solute and substrate, are considered; in the latter case, the bulk solute phase may be pictured as sitting on the surface of the substrate. In each case, oxygen is allowed to adsorb on either one, both, or none of the resulting surfaces. Additionally, separations that result in the formation of both surface alloys (with or without adsorbed oxygen) and stoichiometrically appropriate quantities of solute and host bulk oxides are considered; the free energies of the bulk oxides are taken from experimental data.[27] In this manner, the free energies of all of the above phase separation processes are determined, as functions of the electrode potential, and the potential range over which the surface alloy of interest is stable is identified.

**Supporting Information Available:** Table S1, a complete listing of the calculated oxygen binding energies on all binary surface alloys considered in this study. This information is available free of charge via the Internet at http://pubs.acs.org.

## References and Notes

(1) Greeley, J.; Jaramillo, T.; Bonde, J.; Chorkendorff, I.; Nørskov, J. K. *Nat. Mater.* **2006**, *5*, 909.
(2) Greeley, J.; Nørskov, J. K. *Surf. Sci.* **2007**, *601*, 1590.
(3) Greeley, J.; Mavrikakis, M. *Nat. Mater.* **2004**, *3*, 810.
(4) Andersson, M. P.; Bligaard, T.; Kustov, A.; Larsen, K. E.; Greeley, J.; Johannessen, T.; Christensen, C. H.; Nørskov, J. K. *J. Catal.* **2006**, *239*, 501.
(5) Toulhoat, H.; Raybaud, P. *J. Catal.* **2003**, *216*, 63.
(6) Linic, S.; Jankowiak, J.; Barteau, M. A. *J. Catal.* **2004**, *224*, 489.
(7) Nikolla, E.; Holewinski, A.; Schwank, J.; Linic, S. *J. Am. Chem. Soc.* **2006**, *128*, 11354.
(8) Studt, F.; Abild-Pedersen, F.; Bligaard, T.; Sorensen, R. Z.; Christensen, C. H.; Norskov, J. K. *Science* **2008**, *320*, 1320.
(9) Alayoglu, S.; Nilekar, A. U.; Mavrikakis, M.; Eichhorn, B. *Nat. Mater.* **2008**, *7*, 333.
(10) Stamenkovic, V. R.; Mun, B. S.; Mayrhofer, K. J. J.; Ross, P. N.; Markovic, N. M. *J. Am. Chem. Soc.* **2006**, *128*, 8702.
(11) Stamenkovic, V.; Fowler, B.; Mun, B. S.; Wang, G.; Ross, P. N.; Lucas, C. A.; Markovic, N. M. *Science* **2007**, *315*, 493.
(12) Zhang, J. L.; Vukmirovic, M. B.; Sasaki, K.; Nilekar, A. U.; Mavrikakis, M.; Adzic, R. R. *J. Am. Chem. Soc.* **2005**, *127*, 12480.
(13) Calvo, S. R.; Balbuena, P. B. *Surf. Sci.* **2007**, *601*, 4786.
(14) Gasteiger, H. A.; Kocha, S. S.; Sompalli, B.; Wagner, F. T. *Appl. Catal., B* **2005**, *56*, 9.
(15) Hammer, B.; Hansen, L. B.; Nørskov, J. K. *Phys. Rev. B* **1999**, *59*, 7413.
(16) Greeley, J.; Nørskov, J. K. *Surf. Sci.* **2005**, *592*, 104.
(17) Bengtsson, L. *Phys. Rev. B* **1999**, *59*, 12301.
(18) Vanderbilt, D. *Phys. Rev. B* **1990**, *41*, 7892.
(19) Kresse, G.; Furthmuller, J. *Comput. Mater. Sci.* **1996**, *6*, 15.
(20) Nørskov, J. K.; Rossmeisl, J.; Logadottir, A.; Lindqvist, L.; Kitchin, J. R.; Bligaard, T.; Jonsson, H. *J. Phys. Chem. B* **2004**, *108*, 17886.
(21) Stamenkovic, V.; Mun, B. S.; Mayrhofer, K. J. J.; Ross, P. N.; Markovic, N. M.; Rossmeisl, J.; Greeley, J.; Nørskov, J. K. *Angew. Chem., Int. Ed.* **2006**, *45*, 2897.
(22) Shao, M.; Liu, P.; Zhang, J.; Adzic, R. *J. Phys. Chem. B* **2007**, *111*, 6772.
(23) Hammer, B.; Nørskov, J. K. *Surf. Sci.* **1995**, *343*, 211.
(24) Mavrikakis, M.; Hammer, B.; Nørskov, J. K. *Phys. Rev. Lett.* **1998**, *81*, 2819.
(25) Greeley, J.; Nørskov, J. K.; Mavrikakis, M. *Annu. Rev. Phys. Chem.* **2002**, *53*, 319.
(26) Ruban, A. V.; Skriver, H. L.; Nørskov, J. K. *Phys. Rev. B* **1999**, *59*, 15990.
(27) *CRC Handbook of Chemistry and Physics*, 76th ed.; CRC Press: Boca Raton, FL, 1996.

(28) Strmcnik, D.; Tripkovic, D.; van der Vliet, D.; Chang, K. C.; Komanicky, V.; You, H.; Karapetrov, G.; Greeley, J.; Stamenkovic, V.; Markovic, N. M. *J. Am. Chem. Soc.* **2008**, *130*, 15332.

(29) Srivastava, R.; Mani, P.; Hahn, N.; Strasser, P. *Angew. Chem., Int. Ed.* **2007**, *46*, 8988.

(30) Babu, P. K.; Lewera, A.; Chung, J. H.; Hunger, R.; Jaegermann, W.; Alonso-Vante, N.; Wieckowski, A.; Oldfield, E. *J. Am. Chem. Soc.* **2007**, *129*, 15140.

(31) Greeley, J.; Nørskov, J. K. *Electrochim. Acta* **2007**, *52*, 5829.

(32) Bollinger, M. V.; Jacobsen, K. W; Nørskov, J. K. *Phys. Rev. B* **2003**, *67*, 085410.

(33) Rossmeisl, J.; Norskov, J. K.; Taylor, C. D.; Janik, M. J.; Neurock, M. *J. Phys. Chem. B* **2006**, *110*, 21833.

(34) Greeley, J.; Mavrikakis, M. *Surf. Sci.* **2003**, *540*, 215.

(35) Humphrey, W.; Dalke, A.; Schulten, K. *J. Mol. Graphics* **1996**, *14*, 33.

JP808945Y